Adsorption of anionic dyes from aqueous solution using polyelectrolyte PDADMAC-modified-montmorillonite clay

Rachid Ait Akbour[a,*], Jamila El Gaayda[a], Fatima Ezzahra Titchou[a], Aïcha Khenifi[b], Hanane Afanga[a], Abdelfettah Farahi[c], Pow-Seng Yap[d], Marcus Bruno Soares Forte[e], Mohamed Hamdani[a]

[a]*Physical Chemistry and Environment Team, Faculty of Sciences, University of Ibn Zohr, Agadir, Morocco, email: r.aitakbour@uiz.ac.ma (R.A. Akbour)*

[b]*Laboratory Physical Chemistry of Materials, Catalysis and Environment, Faculty of chemistry, USTOMB, Oran El M'Nouar, Algeria*

[c]*Catalysis and Environment Team, Faculty of Sciences, University of Ibn Zohr, Agadir, Morocco*

[d]*Department of Civil Engineering, Xi'an Jiaotong-Liverpool University, Suzhou 215123, China*

[e]*Bioprocess and Metabolic Engineering Laboratory (LEMeB), Food Engineering Department (DEA), Faculty of Food Engineering (FEA), University of Campinas (UNICAMP), R. Monteiro Lobato, 80, Campinas, São Paulo 13083-862, Brazil*

ABSTRACT

A novel polyelectrolyte poly diallyl-dimethyl-ammonium chloride (PDADMAC)-modified-montmorillonite was evaluated as low-cost adsorbent material to eliminate anionic dyes, namely congo red (CR) and methyl orange (MO), from the aqueous phases via batch adsorption experiments. The PDADMAC-modified-montmorillonite samples were characterized using X-ray diffraction, Fourier transform infrared, scanning electron microscopy, surface area measurement (Brunauer–Emmett–Teller method), zeta potential, and thermogravimetric analysis techniques. The sorption of anionic dyes on PDADMAC-modified-montmorillonite was studied. The experimental results demonstrated that the adsorption of anionic dye differs when varying pH and temperature values. In the presence of interfering anions (SO_4^{2-}, CO_3^{2-}, and HPO_4^{2-}), a decrease in the CR and MO adsorbed amounts were observed. These results highlight the pertinence of PDADMAC-modified-montmorillonite adsorbent for the removal of organic dyes from water contaminated. For both two anionic dyes, the investigations of sorption kinetics and isotherm model indicated that the adsorption kinetic was described better by the pseudo-first-order model, and the equilibrium data obtained were well-described by the Langmuir model. The removal efficiency of PDADMAC-modified-montmorillonite were beyond 90.7% and 69.2% of CR and MO dyes, respectively, showing that the PDADMAC-modified-montmorillonite can be utilized as an efficient adsorbent for anionic dye removal. The calculated thermodynamic parameters showed the spontaneous sorption of CR and MO on PDADMAC-modified-montmorillonite, and also its endothermic character.

Keywords: Dyes; Clay; Surfactant; Adsorption; Montmorillonite

* Corresponding author.

1. Introduction

Dyes applications have an important place in the industrial sector, whereby they are frequently used in food, paint, textiles, cosmetics, leather, papermaking, and plastics industries [1]. The wastewaters generated by textile industries often contain many dyes with complex chemical structures. In general, there are three classes of dyes: non-ionic dyes (disperse dyes), anionic dyes (acid and reactive dyes), and cationic dyes (basic dyes) [2,3]. These substances have adverse impacts on public and animals' health and also aquatic organisms related to their low biodegradability and high toxicity [4,5].

For example, wastewaters discharge of industries contains the anionic colorants, such as congo red, methyl orange, and acid red 57. Their presence in the environment can produce a reduction in oxygen solubility and an enormous risk to human's health, such as skin and mucous membrane irritation and burns [6]. To address these diseases and protect the ecosystem, it is therefore necessary to degrade these discharges before they are discharged into the environment. In this context, several treatment processes have been employed for dye removal including electrochemical oxidation, magnetic separation, coagulation–flocculation, nanofiltration, biodegradation, photocatalytic, and photochemical degradation [7,8], and adsorption [9,10]. However, the adsorption technique seems to be the most advantageous for the elimination of toxic dyes and other chemical pollutants from water and wastewater. Many solid supports as adsorbents have been tested using adsorption techniques for dyes, such as activated carbon [11], kaolin [12], layered double hydroxides [13], and cellulosic materials [14]. A large number of research works have demonstrated that the activated carbon is the most successful and effective adsorbent, despite being expensive due to its high manufacturing and regeneration costs [15]. Hence, it is necessary to find an adsorbent that is effective and easily available as an alternative adsorbent for dye treatment.

Some adsorbents such as natural clay and modified clay have been employed for basic and acid dyes removal respectively, from industrial wastewater [16,17]. Some researchers have used bentonite as a natural mineral adsorbent, which showed high adsorption efficiency of positively-charged dyes, due to its cheapness and chemical properties, for example, high cation-exchange capacity (CEC), specific surface area, and tendency to retain water or other polar and non-polar compounds [18]. In contrast, another study has indicated that bentonite clay has a weak retention capacity of negatively charged anionic dyes [17]. Recently, the improvement of modified bentonite performance for anionic dyes adsorption has been reported by several studies thus, confirming high adsorption efficiency [17]. In many works, the surfactant-modified clays and polymer-modified clays have better adsorption capacity compared to the original clays [19].

For example, Kang et al. [20] revealed that poly (epicholorohydrin dimethylamine) modified bentonite significantly ameliorated the adsorption efficiency for anionic dye DFS removal. Similar observation was reported by Liu et al. [21]. They found higher adsorption of brilliant yellow (BY) on poly(2-(acryloyloxy)ethyl) trimethyl ammonium chloride modified bentonite particles. However, only few researches have reported the employment of modified montmorillonite with cationic surface active agents as solid support for anionic dye elimination from wastewater.

The aim of this work is to study the potential of cationic polyelectrolyte PDADMAC-modified-montmorillonite clay as an adsorbent toward the elimination of anionic dyes, namely congo red (CR) and methyl orange (MO), from the aqueous phase. Influence of various parameters, such as solution pH, temperature, interfering anions introduced in the aqueous solution, and the adsorbent dosage, on the dye elimination were studied. The adsorption data of dyes with PDADMAC-modified-montmorillonite was analyzed utilizing three kinetic models, namely the pseudo-first-order, pseudo-second-order, and intra-particle diffusion. Finally, the results obtained were compared using three isotherm equations, namely Langmuir, Freundlich and Dubinin–Radushkevich.

2. Materials and methods

2.1. Dyes

Two different anionic dyes used in the work were CR and MO. The commercial dyes were supplied by Sigma-Aldrich (France). In this work, the dyes employed were not purified. The chemical structures and characteristics of CR and MO dyes are presented in Table 1.

Table 1
Chemical structures of the studies dyes

Name	Molecular structure	Nature	λ_{max} (nm)
Methyl Orange 52		Anionic	461
Congo Red		Anionic	497

2.2. Montmorillonite particles

The montmorillonite powder was provided from Sigma-Aldrich. The chemical composition of the clay is shown in Table 2, which contain principally SiO_2 and Al_2O_3.

The cation exchange capacity (CEC) was determined using conductimetric method as 102 meq/100 g of montmorillonite according to calculations by Bartelt-Hunt et al. [22]. This method was based on exchanged species and was described by Khenifi et al. [23]. The average diameter (d_{50}) of the unmodified montmorillonite particles was determined from laser granulometry (Malvern Instrument), and the d_{50} value was about 50 μm (Fig. 1).

This clay has undergone a pretreatment with an excess of Na^+ cation representing 10 times the CEC of montmorillonite to ensure that only the Na^+-exchanged is located in the interlayer space. Subsequently, the montmorillonite saturated with Na^+ cation will be modified by cationic polyelectrolyte.

2.3. Cationic polyelectrolyte: poly(diallyl-dimethyl-ammonium chloride)

The polymer employed to change the surface of montmorillonite is a cationic polyelectrolyte, poly(diallyl-dimethyl-ammonium chloride), PDADMAC, with chemical formula $(C_8H_{16}NCl)n$ (CAS Number 26062-79-3), and it was provided by Sigma-Aldrich. Its chemical structure is presented in Fig. 2.

2.4. Reagents

All chemical reagents employed in this study were of analytical grade. The aqueous solutions were prepared using fresh bidistilled water. The ionic strength was fixed using sodium chloride (NaCl). The pH of the aqueous solution was adapted to the suitable pH values by using solutions of HCl or NaOH (0.1M) and indicated by a pH meter (Mettler Toledo, France). Dye solutions with pH 6 were used in all adsorption experiments unless otherwise mentioned. Aqueous solutions of sodium chloride (NaCl), sodium nitrate ($NaNO_3$), sodium sulfate (Na_2SO_4), and sodium carbonate (Na_2CO_3) were prepared and used to study the competing effect of inorganic anion on dyes adsorption onto PDADMAC-modified-montmorillonite.

2.5. Preparation of PDADMAC-modified-montmorillonite

The PDADMAC-modified-montmorillonite was formulated by exchanging the inorganic cation present in the interlayer space of montmorillonite with a cationic polyelectrolyte PDADMAC at 100% of the clay's CEC correspond to the approach reported earlier [22]. The quantity of organic cation added to the montmorillonite was calculated according to Eq. (1) [23]:

$$f = \frac{m_{cation}}{(CEC)(X)m_{clay}MV_{cation}} \tag{1}$$

where f is the fraction of CEC satisfied by organic cation (dimensionless), m_{cation} is the mass of organic cation required to achieve 100% of CEC (mass), CEC of clay (equivalents/mass), X is the moles of charge per equivalent (mol/equivalent), m_{clay} is the mass of clay (mass), and MW_{cation}: gram molecular weight of organic cation (mass/mol).

The preparation of PDADMAC-modified-montmorillonite was carried out in a closed reactor using this procedure: 20 g of sodium montmorillonite was first dispersed into 200 mL distilled water to swell the clay for 60 min. Under stirring, a desired amount of poly(diallyl-dimethyl-ammonium chloride) was added gradually into the slurry of sodium montmorillonite at 66°C. The concentrations of PDADMAC were from 20 to 100 CEC of montmorillonite. Then, the mixture was stirred at 66°C for 180 min. The PDADMAC-modified-montmorillonite complex was filtered and washed several times with distilled
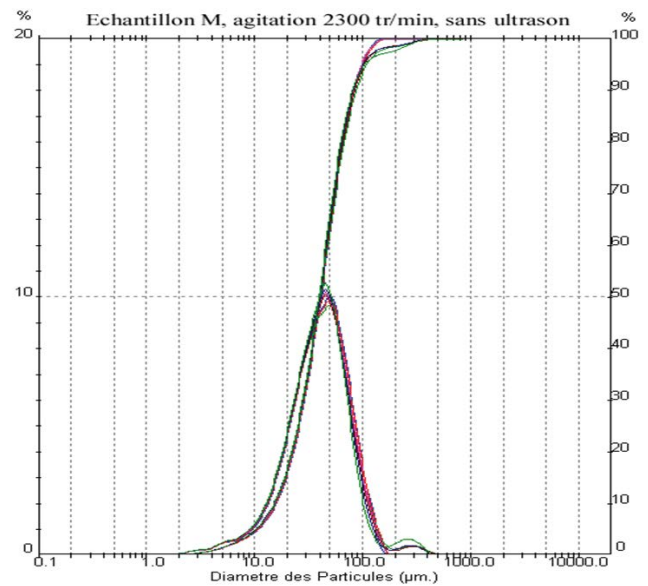
Fig. 1. Distribution of granulometry of montmorillonite.
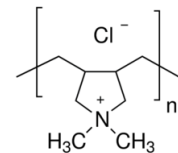
Fig. 2. Chemical structure of polyelectrolyte PDADMAC was used in this study.

Table 2
Chemical composition of montmorillonite

Component	SiO_2	Al_2O_3	Fe_2O_3	Na_2O	MgO	CaO	K_2O	TiO_2
Weight %	60	18	7	3	2	2.1	0.5	1.5

water. The obtained product was oven-dried at 80°C and activated for 60 min at 105°C, and finally grounded in an agate mortar, and stored for further use.

2.6. Characterization methods

The solid samples (the sodium montmorillonite and the PDADMAC-modified-montmorillonite) were analyzed using X-ray diffraction (XRD), Fourier transform infrared (FTIR), scanning electron microscopy (SEM), surface area measurement (BET method), zeta potential, and thermogravimetric analysis (TGA) techniques, in order to get further insights into PDADMAC-modified-montmorillonite structure, functional groups, and surface properties.

The XRD data of the solid were collected with a PANalytical's X'Pert PRO diffractometer (France). The attenuated total reflectance infrared spectra (ATR-FTIR) were collected on an FTIR Nicolet 5700 (Thermo Electron Corporation, USA) spectrometer equipped with a Smart Orbit accessory.

The surface morphology and microstructure of sodium montmorillonite and PDADMAC-montmorillonite samples were observed by scanning electron microscopy SEM technique (PHILIPS SEM 525M, France). The SEM analyses were conducted under accelerating voltage at 30 kV.

The specific surface area and average pore size of the sodium montmorillonite and PDADMAC-montmorillonite particles were determined by N_2 gas adsorption–desorption technique at 77 K using a Micromeritics ASAP2000 surface analyzer and were calculated by Brunauer–Emmett–Teller (BET) method.

TGA analyses of sodium montmorillonite and PDADMAC-montmorillonite samples were performed on a Setaram Instrumentation (Setsys Evolution, France). The zeta potential of PDADMAC-montmorillonite particles was measured by microelectrophoresis using a ZetaSizer Nanoseries (Malvern Instrument).

2.7. Adsorption experiments

The adsorption tests were performed which implies that the batch method in a 250 mL Erlenmeyer flask, and were conducted with a fixed amount of the PDADMAC-modified-montmorillonite in 100 mL of different dye solution at a steady agitation speed. The kinetic experiments were conducted to evaluate and to compare adsorption rates of MO and CR dyes on adsorbent. For this, 0.1g of PDADMAC-modified-montmorillonite was added to 100 mL of dye solution of 130 mg/L. Experiments were conducted at pre-determined time interval.

These series of experiments were carried out at natural pH = 6.5, at an ionic strength of 10^{-2} M of NaCl, at ambient temperature.

In another series of experiments examining the effect of the pH of the aqueous phase and nature of the interfering anions present in the solution, an equal amount of adsorbent (0.1 g organo-montmorillonite) was introduced in erlenmeyer flask and 100 mL of salt solutions containing various amounts of dyes (initial dye concentration varying from 10 to 150 mg/L), was added at ambient temperature.

The effect of pH on dyes was examined by fixing the dyes solutions (1,000 mg/L) desired pH values (3, 4, 6.5, 9,

and 11) using HCl (1 N) or NaOH (1 N) and stirring 100 mL of dye solution with 0.1 g adsorbent at room temperature and at NaCl concentration equal to 10^{-2} M.

The influence of interfering anion nature was evaluated by adding various salts (NaCl, Na_2SO_4, Na_2CO_3, and $NaHPO_4$) to the dispersions at fixed salt concentration of 10^{-2} M at pH = 6.5. The interfering anions adopted to examine this effect are chloride, sulfate, hydrogen phosphate, and carbonate. The selection of these anions is due to their predominance in the soils and groundwaters.

For adsorption isotherm experiment, the sample was rapidly centrifuged at 4,000 rpm for 15 min. The residual dye concentrations were estimated by measuring the absorbance of supernatant using a UV-vis spectrophotometer. The absorbances at a specific wavelength were measured for MO (λ = 461 nm), and CR (λ = 497 nm), for each dye, where the calibration curves were established.

The adsorbed quantity, Q_{ads}, as expressed in milligram of dye per gram of the solid, and the dye removal efficiency, were calculated using the equations, respectively:

$$Q_{ads} = \left(C_i - C_e \right) \times \frac{V}{m} \tag{2}$$

$$\%\text{Removal efficiency} = \left(\frac{C_i - C_e}{C_i} \right) \times 100 \tag{3}$$

where m is the amount of the PDADMAC-modified-montmorillonite adsorbent (g), V is the volume of dye solution (L), C_i and C_e are initial and residual dye concentrations, respectively (mg/L).

To evaluate the impact of temperature on dyes removal, the dispersions aqueous containing 0.1 g adsorbent and 130 mg/L of dye at natural pH, were stirring at 293, 313, and 333 K, respectively. The dispersions obtained were mixed for a contact time varying from 10 to 120 min. The collected fractions were centrifuged and analyzed for determining the dye adsorbed quantity, using the same procedures described previously.

3. Theory section

3.1. Adsorption kinetic models

So as to investigate the behavior of adsorption process of dyes onto our adsorbent, the data obtained experimentally were fitted by three kinetics models namely pseudo-first-order model [24], pseudo-second-order model [25], and intraparticle diffusion model [26]. The pseudo-first-order model is given by Eq. (4):

$$\frac{dq(t)}{dt} = k_1 \times \left(q_e - q(t) \right) \tag{4}$$

where $q(t)$ and q_e are, respectively, the amounts adsorbed per unit mass of the adsorbent (both in mg/g) at any time and at equilibrium, and k_1 is the pseudo-first-order rate constant of adsorption (1/min). The linearized form of equation (Eq. (4)) is expressed by Eq. (5):

$$\ln\left(q_e - q_t\right) = \ln q_e - k_1\left(t\right) \tag{5}$$

The pseudo-second-order model is expressed as Eq. (6):

$$\frac{dq\left(t\right)}{dt} = k_2 \times \left(q_e - q\left(t\right)\right)^2 \tag{6}$$

where k_2 is the rate constant of pseudo-second-order adsorption. Integration of this equation (Eq. (6)) gives equation (Eq. (7)):

$$q\left(t\right) = \frac{k_2 q_e^2 t}{1 + k_2 q_e t} \tag{7}$$

Intra-particle diffusion model:

The intra-particle diffusion model used to study the diffusion in the adsorption system is originated from Fick's second law and is written as Eq. (8) [27]:

$$q\left(t\right) = K_i t^{0.5} + C_{ste} \tag{8}$$

where K_i is the intra-particle diffusion rate constant (mg/g/min$^{0.5}$) and C_{ste} (mg/g) is a constant.

3.2. Adsorption models

The experimental data obtained were analyzed using several isotherm models to determine the best-fit isotherm and confirm the adsorption mechanism. For each dye, the equilibrium adsorption data were interpreted using three different mathematical models, that is, Langmuir [28], Freundlich [29], and Dubinin–Radushkevich (D–R) [30], which are represented by the following equations, respectively:

$$q_e = \frac{q_m K_L C_e}{1 + K_L C_e} \tag{9}$$

$$R_L = \frac{1}{1 + K_L C_0} \tag{10}$$

$$q_e = K_F \times C^{\frac{1}{n}} \tag{11}$$

$$q_e = q_m e^{-\beta \varepsilon^2} \tag{12}$$

$$\varepsilon^2 = RT \ln\left(1 + \frac{1}{C_e}\right) \tag{13}$$

where q_e (mg/g) is the amount of dye adsorbed at equilibrium, C_{eq} is the equilibrium dye concentration in aqueous phase (mg/L), K_L is Langmuir equilibrium constant (L/mg), and q_m the maximum adsorption capacity (mg/g). R_L is dimensionless separation constant.

where K_F (L/mg) and $1/n$ are the Freundlich constants. ε is the Polanyi potential, and β (mol^2.kJ^{-2}) is a constant related to the mean free energy of adsorption.

3.3. Adsorption thermodynamics

The thermodynamic parameters for adsorption of two dyes onto PDADMAC-modified-montmorillonite particles were determined consecutively to experimental data collected at different temperatures and were given by using the following equations:

$$\Delta G° = -RT \ln\left(K_d\right) \tag{14}$$

where $\Delta G°$ is the standard Gibbs free energy change (J/mol), R is the universal gas constant (8.314 J/mol K), T is the absolute temperature (°K), and K_d is the distribution coefficient given by equation:

$$\ln\left(K_d\right) = \frac{-\Delta H°}{RT} + \frac{-\Delta S°}{R} \tag{15}$$

where $\Delta H°$ and $\Delta S°$ are the enthalpy and entropy of adsorption reaction, respectively. The values of $\Delta H°/R$ and $\Delta S°/R$ can be evaluated from the slope and the intercept of the van't Hoff plot of $\ln(K_d)$ vs. $1/T$ respectively.

4. Results and discussion

4.1. Characterization of adsorbent

XR diffractograms of the PDADMAC-modified-montmorillonite samples are presented in Fig. 3. A displacement of the 001 diffraction peak toward small angles values was observed. This result shows a widening of the inter-lamellar space and allocated to the intercalation of PDADMAC polyelectrolyte chains. Table 3 summarizes the interlayer distance of sodium montmorillonite and PDADMAC-modified-montmorillonite samples at different PDADMAC concentration. It was found that the interlayer spacing increased gradually with PDADMAC polyelectrolyte addition.
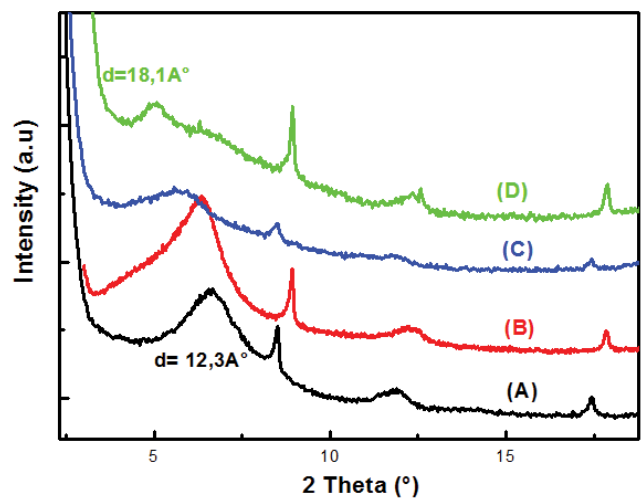
Fig. 3. XRD spectra of unmodified montmorillonite (A), PDAD-MAC-modified- montmorillonite with PDADMAC of 30 (B), 50 (C), and 100 (D) CEC of montmorillonite.

Table 3
Interlayer distance of sodium montmorillonite and PDADMAC-modified-montmorillonite as function of PDADMAC concentration

PDADMAC concentration used in preparation PDADMAC-modified-montmorillonite following percentage of the clay's CEC (% CEC)					
CEC %	0 (Sodium montmorillonite)	20	30	50	100
d(001) (Å)	12.3	13.6	14.2	15.50	18.1

The XRD patterns of sodium montmorillonite and montmorillonite modified with cationic polymer (PDADMAC) equivalent to 100% the CEC of initial montmorillonite are presented in Fig. 4a. The (001) basal reflection of the montmorillonite particles situated at 6.5°, which corresponded to the interlayer basal-spacing of 12.3 Å [31,32] indicating that natural montmorillonite is rich in sodium cation. When montmorillonite was modified with PDADMAC, a strong reflection at 4.6° appeared, corresponding to a higher d-spacing of 18.1 Å. The expansion of the d-spacing of montmorillonite modified with cationic polymer was likely attributed to the incorporation of PDAPMAC cations into the montmorillonite structure through intercalation within the interlamellar space, and replacement of inorganic layer cations and their hydration water molecules with PDAPMAC chains. In addition, this modification was ascribed to the fixation of the positively charged ammonium groups of PDADMAC polyelectrolyte into the aluminol (>Al–O$^-$) and silanol (>Si–O$^-$) groups of the surface, which are dissociated, via the electrostatic interactions. In aqueous phase, the adsorption of surfactants at the clay – water interface is dominated principally by electrostatic and hydrophobic interactions [33] including both the interaction between the surfactant and the mineral surface, and the mutual interaction between surfactant molecules. This behavior will be proven by other analysis techniques such as FTIR, SEM, and microelectrophoresis.

The FTIR spectra of sodium montmorillonite and PDADMAC-montmorillonite are shown in Fig. 4b. The bands at 3,625 and 3,415 cm^{-1} in the FTIR spectrum are typical to montmorillonite, and they can be ascribed to the structural OH vibration and stretching vibration of the H–O–H, respectively [34]. In addition, the bands at 1,030; 523; and 464 cm^{-1} were attributed to the stretching vibration of Si–O, bending vibration of Si–O–Al and Si–O–Si, respectively [35]. The band at 1,640 cm^{-1} is ascribed to the H–O–H bending vibration within the clay interlayer [36]. Comparison between the two spectra shows that the intensity of this band decreased after contacting sodium montmorillonite with PDADMAC solution due to the replacement of H$_2$O with polyelectrolyte. Therefore, the surface properties of PDADMAC-modified-montmorillonite changed from a hydrophilic to a hydrophobic character. In addition, the FTIR spectrum of PDADMAC-modified-montmorillonite showed two bands at 2,851 and 2,921 cm^{-1}, and this could be ascribed to the symmetric and anti-symmetric CH$_2$ stretching vibrations, respectively [32].

FTIR spectra analysis well confirms the results of the X-ray analysis, thus indicating that the montmorillonite was well modified by PDADMAC polyelectrolyte under the experimental conditions used.

The SEM images of sodium montmorillonite and PDADMAC-modified-montmorillonite are shown in Figs. 4c and d, respectively. The surface morphology of montmorillonite clay was altered after contacting with PDADMAC surfactant. Indeed, the montmorillonite particles have a quite slick and non-regulated surface with different sizes of block structure (Fig. 4c). On the other hand, the surface morphology of PDADMAC-modified-montmorillonite sample has a rough surface with a small number of pits (Fig. 4d).

The nitrogen adsorption–desorption at 77 K experiments were carried out to determine the specific surface areas as well as the average pore diameter values of both montmorillonite and PDADMAC-montmorillonite samples. The values calculated from the BET method are presented in Table 4 indicates that the specific surface areas of montmorillonite and PDADMAC-modified-montmorillonite samples are 80.12 and 34.32 m^2/g, respectively. The observed decrease in specific surface areas of montmorillonite after modification with PDADMAC can be related to the intercalation of PDADMAC surfactant in the montmorillonite structure where the interlayer space of montmorillonite prevents the migration of nitrogen molecules through the internal surface [37]. However, the average pore diameter of PDADMAC-modified-montmorillonite is 9.42 nm liken to 5.32 nm of montmorillonite.

The thermogravimetric curves of sodium montmorillonite and PDADMAC-modified-montmorillonite were shown in Fig. 4e. Two mass loss levels for temperature below 150°C and between 400°C and 650°C were observed. These losses correspond to the vaporization of water molecules that solvates interlayer cations and dehydroxylation of the structural OH units of montmorillonite clay, respectively. For montmorillonite treated by PDADMAC, the curve shows lower mass loss below 150°C, related a net decrease of the water loss as a result of the replacement of water molecules with polymer chains in the solvatations shell of Na cations into the interlayer space. In addition, a significant loss of mass is observed within the temperature field of 400°C–600°C, and this can be attributed to the decomposition of PDADMAC.

The zeta potential curves of sodium montmorillonite and PDADMAC-modified-montmorillonite particles in water as function of solution pH are presented in Fig. 4f. It is shown that the montmorillonite particle alone has negative zeta potential and these values increases in magnitude with the increase of solution pH. These negatives values denote that the montmorillonite particle surface is negatively charged in all the pH range studied. This behavior is associated with isomorphous substitutions in the mineral lattice by causing permanent negative charges the clay particle surface [38]. The surface charge of sodium
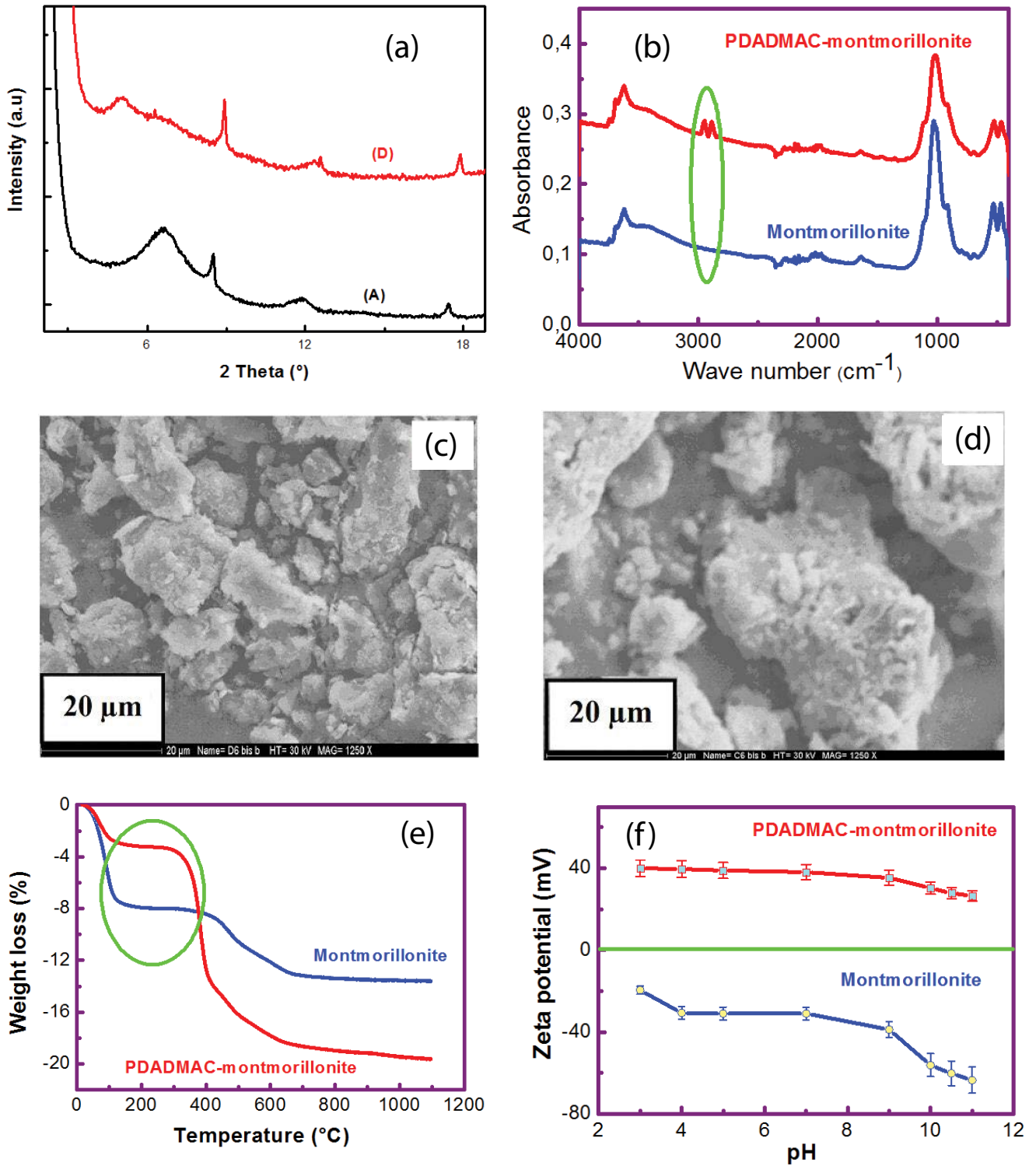
Fig. 4. (a) XRD spectra of unmodified montmorillonite (A), PDADMAC-modified- montmorillonite with PDADMAC 100 CEC of montmorillonite (D), (b) IR spectra of unmodified montmorillonite and PDADMAC-modified- montmorillonite, (c) SEM picture of unmodified montmorillonite, (d) SEM picture of PDADMAC-modified-montmorillonite, (e) Thermogravimetric curves of unmodified montmorillonite and PDADMAC- modified-montmorillonite and (f) the variation of zeta potential of unmodified montmorillonite and PDADMAC- modified-montmorillonite in function of pH.

montmorillonite modified by cationic polymer becomes positive due to the adsorption of PDADMAC ammonium groups on montmorillonite negative surface sites by electrostatic interactions. In addition, the zeta-potential values for PDADMAC-modified-montmorillonite decrease slightly in magnitude with increasing pH from 3 to 11 but remain positive (Fig. 4f). This decrease can be associated with the compensation of PDADMAC-modified-montmorillonite positive charge surface sites by OH^- ions. In addition, it is noted that the zeta potential values of raw montmorillonite and modified montmorillonite were less than –30 mV and greater than +30 mV, respectively. This implies that the PDADMAC-modified-montmorillonite particles dispersion system was relatively stable in the aqueous phase [39].

All of the analysis results demonstrated that montmorillonite is well-modified by the PDADMAC organic cation, as well as its surface properties. Consequently, this modification will lead to the improvement of its capacity for the removal of anionic dyes from the solution; and this will be demonstrated later on in this work.

4.2. Effect of contact time

The effect of the contact time on the adsorption process of dye (MO and CR) onto PDADMAC-modified-montmorillonite (organo-montmorillonite) (Fig. 5a) was studied. The results of the adsorption kinetics study are shown in Fig. 5a. The data shows the adsorption equilibrium

Table 4
Calculated parameter from BET method of used samples

Samples	Surface area (m^2/g)	Pore diameter (nm)
Montmorillonite	80.12	5.32
PDADMAC-montmorillonite	34.32	9.42
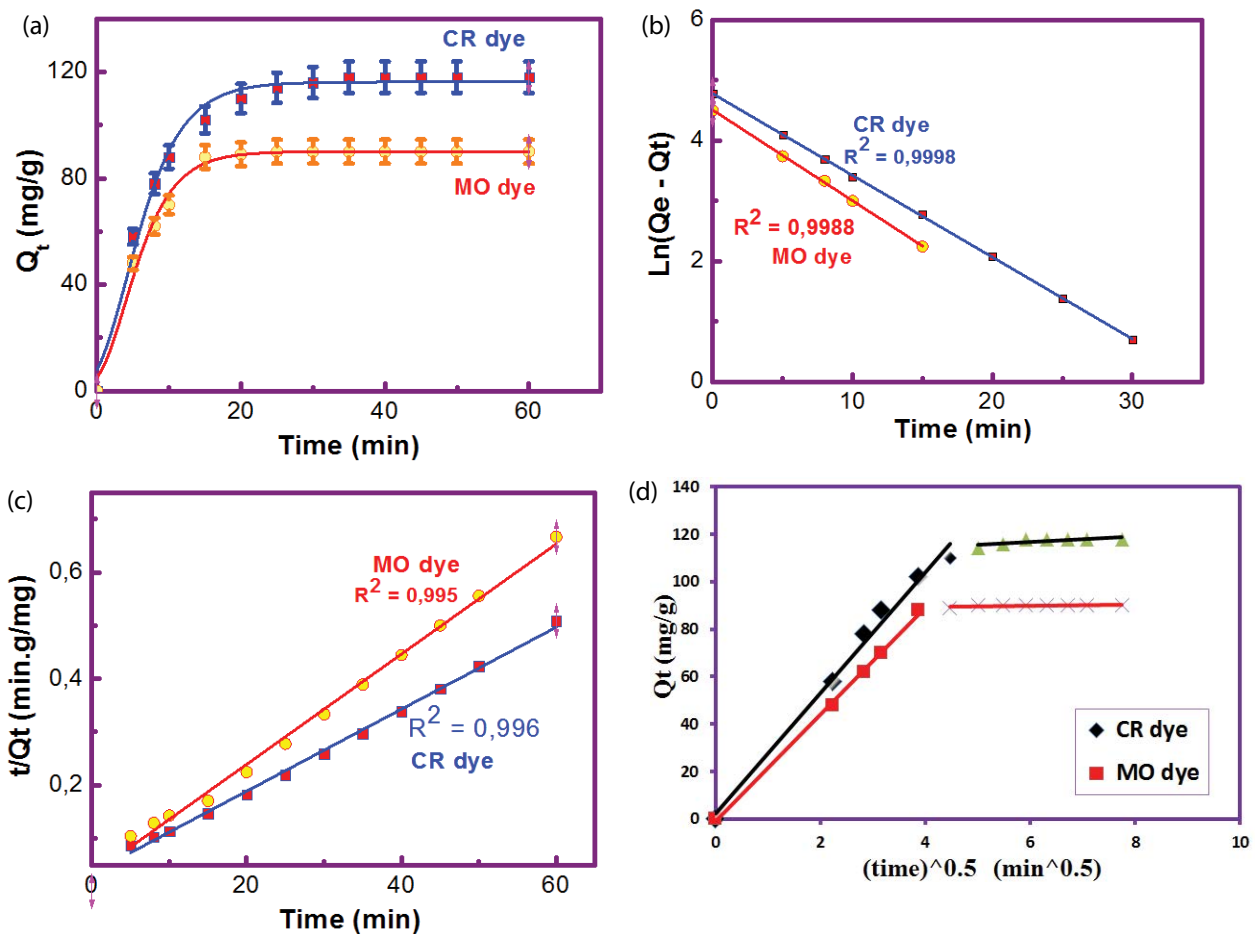
Fig. 5. (a) Adsorption kinetics for CR and MO dyes by PDADMAC-modified-montmorillonite, (b) pseudo-first-order kinetic plots, (c) pseudo-second-order kinetic plots and (d) intraparticle diffusion plots for adsorption CR and MO dyes by PDADMAC-modified-montmorillonite.

for MO and CR on PDADMAC-modified-montmorillonite can be achieved within 15 min of contact time with 118 and 90 mg/g for CR and MO dyes, respectively. This behavior is probably attributed to the density of actives sites onto PDADMAC-modified-montmorillonite surfaces which available at the beginning for the adsorption of dyes. Meanwhile, the saturation of adsorption occurs with contact time due to a decrease of adsorption sites on the adsorbent surface and also to decrease of dye concentration in the solution. Furthermore, the decrease in the adsorption rate can be associated with the formation of a monolayer of dyes molecules on the PDADMAC-modified-montmorillonite surface. Under our experimental conditions, the percentages of dye removal efficiency calculated are 90.76% and 69.23% for CR and MO dyes, respectively. From these results, it was implied that the acid dyes CR and MO have a good affinity toward the basic adsorbent surface. This result proves that the modification of montmorillonite by the PDADMAC organic cation leads to an improvement in the adsorption capacity of the anionic dyes by the clay which was negatively charged. Compared to the unmodified montmorillonite case, the removal percentages of CR and MO dyes are very low, which do not exceed 7% and 5%, respectively (figure not shown). This is due to the repulsive interactions developed between the anionic dyes and unmodified montmorillonite which is also negatively charged. In the next adsorption experiment, the equilibrium time for the adsorption of dyes (CR and MO) onto PDADMAC-modified-montmorillonite particles was 60 min.

The rate constants adsorption of the dyes by the modified montmorillonite for pseudo-first-order and pseudo-second-order models are determined graphically (Figs. 5b and c). For both CR dye-PDADMAC-modified-montmorillonite and MO dye–PDADMAC-modified-montmorillonite systems, the rate constants were calculated from the lines obtained. These rate constants and the correlation coefficient R^2 of the kinetic models are given in Table 5.

According to the constant empirical correlation R^2 value, all models seem applicable to our experimental data. In fact, for both dyes, the correlation coefficient estimated for the pseudo-first-order and pseudo-second-order models are nearby to unity. However, for pseudo-second-order model, the calculated q-values (129.9 and 100 mg/g) are higher as compared to those obtained experimentally (118 and 90 mg/g) for CR dye and MO dye, respectively. Therefore, the pseudo-second-order model was not more adapted to describe the adsorption of both dyes onto PDADMAC-modified-montmorillonite. On the other hand, the pseudo-first-order was better than the pseudo-second-order model to fit adsorption data because the

values of adsorbed amounts at equilibrium ($q_{e,\mathrm{cal}}$ = 118.39 and 89.74 mg/g) are coherent with the experimental results (118 and 90 mg/g) for CR dye and MO dye, respectively. In addition, the rate constants calculated (Table 5) are 0.153 and 0.140 1/min for CR and MO dyes, respectively. It is noted that the rate constant of CR dye adsorption is higher, which correlates with its greater adsorption capacity (q_m). This can be related to the strong affinity of PDADMAC-modified-montmorillonite for the CR dye. The present results are coherent with earlier workers who have reported the eliminate of acid blue 113, ethyl orange and metanil yellow dyes onto carbonaceous adsorbent [40]. In order to verify the applicability of kinetic models, the calculation of the sum of error squares is important and it's determined by the following equation [41]:

$$\mathrm{SSE}\ \% = \frac{\sqrt{\sum\left(q_{e,\mathrm{cal}} - q_{e,\mathrm{exp}}\right)^2}}{N} \tag{16}$$

where N is the number of data points.

From Table 5, the higher value of R^2 and the lower value of SSE determined in the case of pseudo-first-order kinetic model suggest better fitness of the data and indicates that the adsorption follows pseudo-first-order kinetics. Similar results were also reported for the eliminate of industrial dye Supranol Yellow AGL from aqueous samples [42].

The intraparticle diffusion model was employed in this study so as to understand the mechanistic step that controls the sorption behavior of the dye at the PDADMAC-modified-montmorillonite – aqueous solution interface. The intraparticle diffusion plots for adsorption of CR and MO dyes onto modified montmorillonite are illustrated in Fig. 5d. From this Fig. 5, for both cases, the plots have two linear sections corresponding to two steps of adsorption process. This implies that the adsorption phenomenon is done by surface boundary layer diffusion correspond to initial linear segments of the plot and intraparticle diffusion corresponding to second linear portion [42,43]. The correlation coefficients and rate constant values of intraparticle diffusion model are indicated in Table 5. These calculated values are lower than those found for the pseudo-first-order and pseudo-second-order models. The found results propose that the adsorption process is controlled by the contribution of other sorption mechanisms.

4.3. Effect of adsorbent dose

The adsorbent dose effect on adsorption of CR and MO dyes onto PDADMAC-modified-montmorillonite particles

Table 5
Kinetics parameters for adsorption of two dyes on PDADMAC-modified-montmorillonite

Dyes	q_e (exp) (mg/g)	Pseudo-first-order				Pseudo-second-order				Intraparticule diffusion			
		q_e (cal) (mg/g)	k_1 (1/min)	R^2	SSE (%)	q_e (cal) (mg/g)	k_2 (g/mg min)	R^2	SSE (%)	K_i (mg/g min$^{0.5}$)	R^2	K' (mg/g min$^{0.5}$)	R^2
CR	118	118.39	0.153	0.999	0.057	129.87	0.00211	0.996	0.0910	25.46	0.989	1.299	0.609
MO	90	89.74	0.140	0.998	0.060	100	0.00310	0.995	0.0676	22.51	0.998	0.1936	0.357

was examined by varying the adsorbent dose from 0.5 to 1.5 g/L (Fig. 6). The dye removal efficiency increased with increasing PDADMAC-modified-montmorillonite dosage due to the excessive availability of active sites present at higher adsorbent dosage [44]. However, gradual increase in % removal efficiency was observed from 1 to 1.5 g/L of PDADMAC-modified-montmorillonite adsorbent and the percentage removal efficiency (95.67% and 78%) for CR and MO dyes respectively tended to maintain a constant above 1.5 g/L of adsorbent because the adsorption was almost saturated [45]. Hence, the suitable adsorbent quantity of PDADMAC-modified-montmorillonite is 1 g/L for the elimination of CR and MO dyes from aqueous solutions.

4.4. Effect of pH

pH effect on the removal efficiency of two dyes (CR and MO) from the aqueous phase by adsorption into PDADMAC-modified-montmorillonite surface is presented in Fig. 7. The removal efficiency of CR and MO was reduced from 97.4% to 77% and 80.3% to 45%, respectively, with increasing pH from 3 to 11. These results suggested that the adsorption of dyes is dependent on both their charge and the adsorbent surface charge. In fact, the zeta potential measurements carried out have shown that the PDADMAC-modified-montmorillonite particles are positively charged in the studied pH range (Fig. 4f), due to adsorption of PDADMAC cation, especially the ammonium functional groups, onto montmorillonite sites surface negatively charged, indicating the inversion of unmodified montmorillonite surface charge. This implies the role of PDADMAC on unmodified montmorillonite surface charge change.

Furthermore, the greater adsorption capacity of the anionic dyes (CR and MO) onto the adsorbent surface at acidic medium can be allocated to electrostatic interaction between the PDADMAC-modified-montmorillonite sites surface charged positively and the sulfonate groups – SO_3^- of dye charged negatively [46]. In alkaline medium, when the pH of the solution increases, the number of positively charged sites on the PDADMAC-modified-montmorillonite surface decreases as resulting from the OH^- ions adsorption and causing of the reduction of the adsorbed amount of anionic dye. Moreover, the lower adsorption capacity of CR and MO dyes was explained to the presence of excess OH^- which will compete with the anionic dye for the same adsorption sites [47]. These results are similar to earlier findings for the adsorption of anionic dyes onto organo-bentonite [48]. According to these interpretations, the chemisorption mechanism, and electrostatic interactions can be operative.

4.5. Effect of the type of the interfering anions

Anions effect on the adsorption of CR and MO dyes from aqueous phase onto the PDADMAC-modified-montmorillonite was investigated (Fig. 8a). In general, dye removal efficiency is dependent on the types of interfering anions introduced in the aqueous medium. Indeed, the results obtained denote that the adsorption capacity of CR and MO dyes decrease in the order: $SO_4^{2-} > CO_3^{2-} > HPO_4^{2-}$. This behavior of dyes adsorption could be assigned to the affinity of counter-anion toward to PDADMAC-modified-montmorillonite surface and therefore to screening of the solid support particles positive surface charge. The values of zeta potential of PDADMAC-modified-montmorillonite clay particles in presence of SO_4^{2-}, CO_3^{2-}, and HPO_4^{2-} anions are presented in Fig. 8b and indicate a reduce in magnitude of the charge density but it remains positive, ascribed to the electrostatic attraction of the SO_4^{2-}, CO_3^{2-}, and HPO_4^{2-} anions with the PDADMAC-modified-montmorillonite positive surface site.

Within experimental error, we note that the reduction of the zeta potential is important in the presence of HPO_4^{2-} than CO_3^{2-} and SO_4^{2-} and this may be probably be assigned to the anionic charge density. However, the decrease of adsorbed amount of both CR and MO dyes could be related to the competition adsorption between the counter-anions and dyes molecules toward the sites of adsorbent surface which could cause repulsive interactions. This behavior is identical to that found when the solution pH is increased.
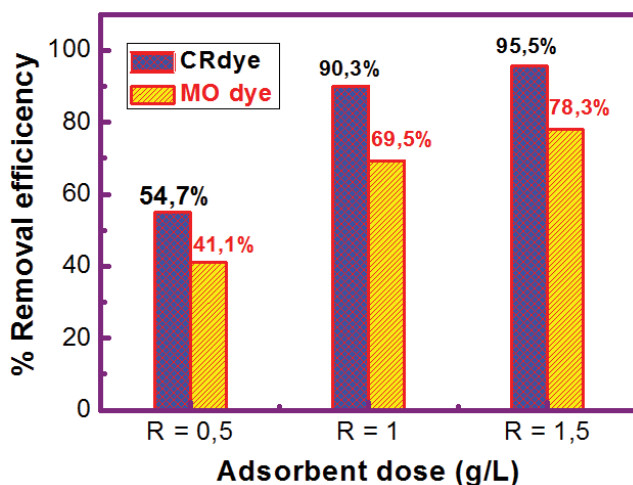
Fig. 6. Effect of adsorbent dose on adsorption of CR and MO dyes onto PDADMAC- modified-montmorillonite.
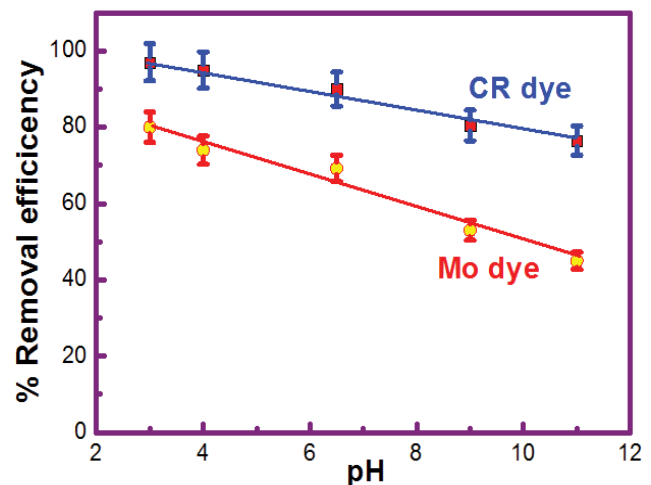
Fig. 7. Effect of pH on the removal efficiency of CR and MO dyes by PDADMAC-modified- montmorillonite.
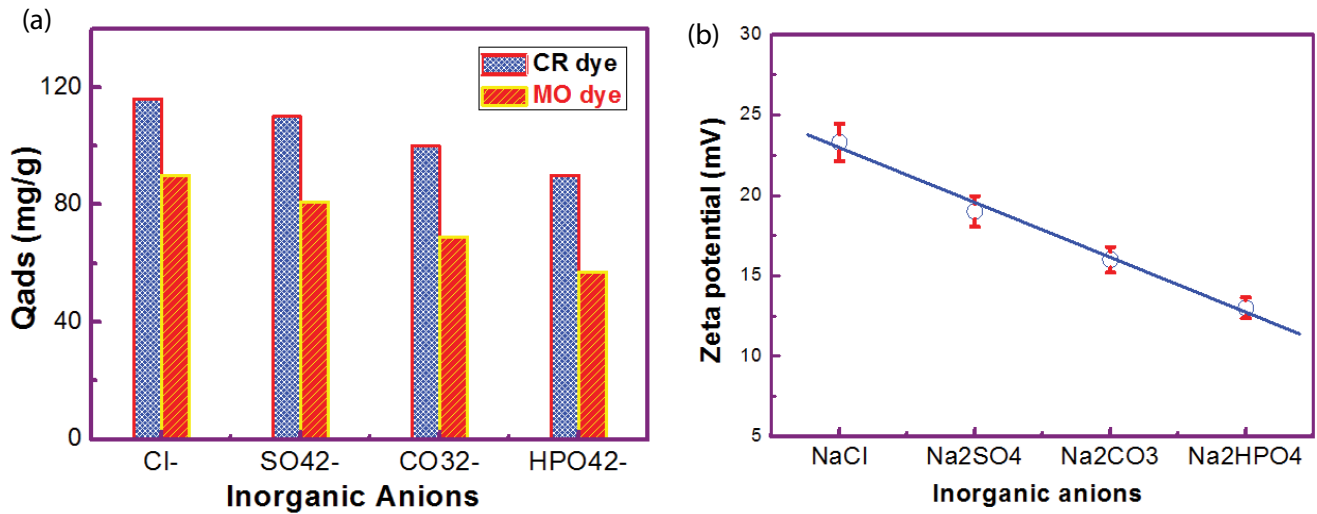
Fig. 8. (a) Effect of dye uptake in the presence of counter-anions. (b) Zeta potential of PDADMAC-modified-montmorillonite in presence of Cl^-, SO_4^{2-}, CO_3^{2-}, and HPO_4^{2-} anions.

4.6. Effect of temperature

Table 6 shows the obtained results of influence of temperature on the adsorption capacity of onto PDADMAC-modified-montmorillonite solid toward each dye. The adsorption capacity of CR and MO dyes on PDADMAC-modified-montmorillonite particles increase with increasing adsorption temperature values from 20°C to 50°C. Indeed, the CR and MO adsorbed amount increased linearly from 118 and 90 to 129 and 102 mg/g, respectively, with an augmentation in the solution temperature. This indicates that the adsorption process is endothermic with chemisorption-like mechanism. Indeed, these results can be due to higher rate diffusion through the boundary layer to the solid surface and large penetration of molecules dyes from the bulk solution phase to PDADMAC-modified-montmorillonite surface [32]. Generally, the increase in the adsorption capacity with the temperature is principally attributed to increase the electrostatic interactions involved between the active sites on the adsorbent and the adsorbate. Furthermore, high temperature promotes a decrease in the viscosity of the aqueous phase which in turn increases the mobility of the adsorbate molecules toward the adsorbent surface [43]. Some authors have been reported that the adsorption of anionic and cationic dyes on surfactant modified clay adsorbent increases with increasing of the solution temperature, concluding that the adsorption is endothermic process [49,50].

The plot of $\ln(K_d)$ against $1/T$ is represented in Fig. 9, and it is a straight line. Hence, $\Delta H°$ and $\Delta S°$ can be estimated from the slope and intercept, respectively.

Furthermore, thermodynamic parameters values obtained are presented in Table 6. As shown in Table 6, the values enthalpy change ($\Delta H°$) in this study are 58.48 and 12.52 kJ/mol for CR and MO dyes, respectively, and are positive. This confirms that the adsorption phenomenon is endothermic in nature. Also, the values of entropy change ($\Delta S°$) are positive indicating an augmentation in randomness at the solid/liquid interface during the adsorption of all dyes on PDADMAC-modified-montmorillonite solid. For CR and MO dyes, the $\Delta G°$ values are negative which implies that the sorption reaction of two dyes is spontaneous and feasible. Furthermore, $\Delta G°$ values decrease from –4.958 to –11.454 kJ/mol for CR dye and from –1.958 to –3.441 kJ/mol for MO dye proposed that the spontaneous nature of the adsorption increases when the temperature was increased from 293 to 323°K. In addition, the values $\Delta G°$ found are between 0 and –10 kJ/mol, implying that the process of

Table 6
Thermodynamic parameters calculated and adsorbed amount of dyes on PDADMAC-modified-montmorillonite particles at various temperature

T (°K)	CR dye				MO dye			
	Q_{ads} (mg/g)	$\Delta H°$ (KJ/mol)	$\Delta S°$ (J/K mol)	$\Delta G°$ (KJ/mol)	Q_{ads} (mg/g)	$\Delta H°$ (KJ/mol)	$\Delta S°$ (J/K mol)	$\Delta G°$ (KJ/mol)
293	118	58.485	216.53	–4.958	90	12.523	49.426	–1.958
303	122			–7.123	94.3			–2.453
313	126			–9.288	98			–2.947
323	129			–11.454	102			–3.441
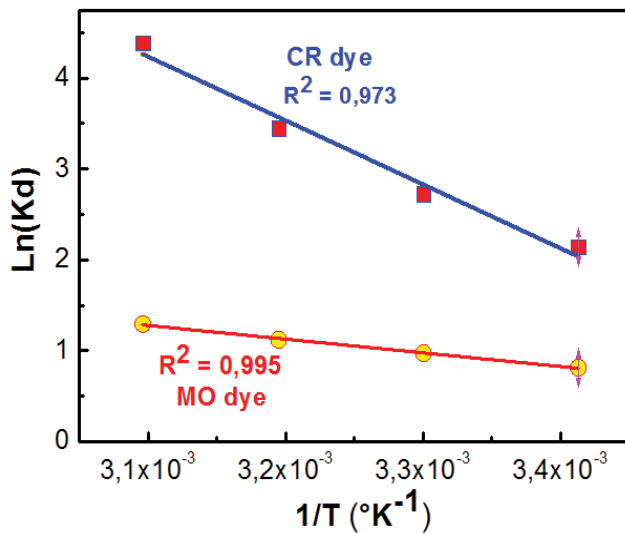
Fig. 9. Plots of Ln*Kd* vs. 1/*T*: Estimation of thermodynamic parameters for the adsorption of CR and MO dyes by PDADMAC-modified-montmorillonite.

adsorption of the CR and MO dyes onto PDADMAC-modified-montmorillonite is attributed to the physisorption process. Our results are right accord with those reported by Chaari et al. [51], on the adsorption of cationic and anionic dyes by smectite rich natural clays.

4.7. Adsorption isotherms

The adsorption isotherms experimental results are illustrated in Fig. 10a. The plots of this figure describe the existing relationship between the amounts of adsorbed quantities of each dye and its concentrations in the equilibrium solution at constant temperature. The adsorbed quantities increase with increasing concentration of CR and MO dyes in the solution and then reach a plateau after equilibrium. This indicates that the CR and MO isotherms are similar to *H*-type according to Giles et al. [52]. The result also showed that the CR and MO adsorption are described by strong ionic adsorbate molecule-adsorbent surface interactions.

The adsorption isotherms of two dyes onto PDADMAC-modified-montmorillonite were fitted with as Langmuir, Freundlich, and Dubinin–Radushkevich models, Eqs. (8), (10), and (11).

The adjustable parameters by linear fitting of Langmuir, Freundlich, and Dubinin–Radushkevich (D–R), and regression coefficients (R^2) are given in Table 7. The linear form of the isotherm equation used are also shown in this table.

The results indicate that the Langmuir model is the best fit of experimental data as compared to the Freundlich and Dubinin–Radushkevich based on the coefficient of correlation values. The values of R^2 lower than 0.95 suggested the modeling performance of Freundlich and Dubinin–Radushkevich models for CR and MO dyes adsorptions were lower than Langmuir model ($R^2 > 0.99$). In addition, the maximum adsorption quantities (q_m) calculated (Table 7) of two dyes by PDADMAC-modified-montmorillonite particles are almost equal to that obtained

experimentally (Figs. 10b and c), which confirms that CR and MO dyes adsorption by modified montmorillonite agrees well with Langmuir model. This suggested that the surface of PDADMAC-modified-montmorillonite is covered by the monolayer of dye and this can be related to electrostatic interaction between the PDADMAC-modified-montmorillonite groups surfaces charged positively and the functional groups of dye molecule charged negatively.

On the other hand, the favorability of CR and MO adsorptions onto PDADMAC-montmorillonite is examined by calculating a dimensionless parameter (R_L) derived from the Langmuir equation (Eq. (11)) (Table 7). The obtained values of R_L below 1 indicated the dyes – modified montmorillonite systems correspond to favorable adsorption processes [49]. In addition, these values which are close to zero which indicated that the adsorption is irreversible due to high of the dyes – PDADMAC-modified-montmorillonite interactions [54].

The comparison of adsorption capacity of PDADMAC-modified-montmorillonite clay with other types adsorbents reported in the recent literature is presented in Table 8.

It is noted that the adsorption capacity of PDADMAC-modified-montmorillonite clay was higher than the majority of adsorbents. Therefore, it can be effectively used as an adsorbent for the removal of CR and MO dyes from the wastewater effluents.

4.8. Adsorption mechanism

The modification of montmorillonite by the canionic polyelectrolyte PDADMAC is due to (i) intercalation of PDADMAC chains in the interlayer spaces (Fig. 4a), and (ii) adsorption of the ammonium group of PDADMAC on the montmorillonite surface, negatively charged, leading to an inversion of its charge which becomes positive (Fig. 4f).

After the contact of the anionic dyes with PDADMAC-modified-montmorillonite, the X-ray diffractograms of the recovered samples show no shift of 001 diffraction peak toward the small angle (2θ) (Fig. 11). This result proves that dye molecules do not seem to penetrate in the interlayer space. It seems that the anionic dyes would adsorb on PDADMAC-modified montmorillonite surface. This adsorption is established through the electrostatic interactions between the sulfates groups of anionic dyes, which are negatively charged, and the positive sites on PDADMAC-modified montmorillonite surface.

The results obtained, both by XRD and zeta potential measurements, suggest that the association between the clay/surfactant/dye is probably occurring according to the following general sequence:

Montmorillonite (clay)	↔PDADMAC-modified montmorillonite (clay-organic polyelectrolyte)	↔PDADMAC-modified montmorillonite - dye
Negative charge	Positive charge	Negative charge

A schematic representation illustrating the mechanism involved in the adsorption process of anionic dye on PDADMAC-modified montmorillonite is given by the Fig. 12.
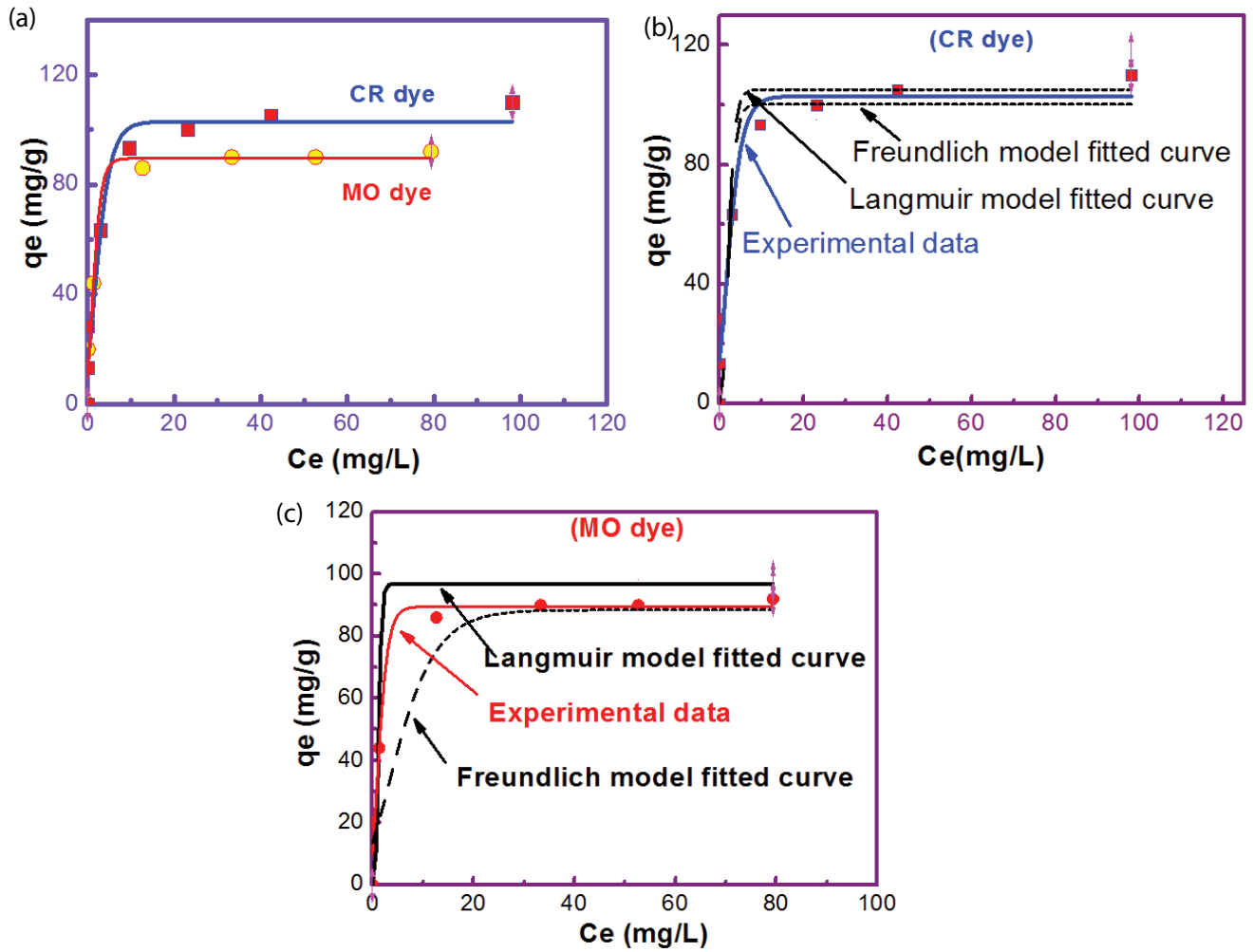
Fig. 10. (a) Adsorption isotherms of CR and MO dyes by PDADMAC-modified- montmorillonite, (b) the nonlinear fitting of Langmuir and Freundlich models for CR dye adsorption onto PDADMAC-modified-montmorillonite and (c) the nonlinear fitting of Langmuir and Freundlich models for MO dye adsorption onto PDADMAC-modified-montmorillonite.

Table 7
Isotherm parameters of Langmuir, Freundlich, and Dubinin–Radushkevich for CR and MO dyes adsorption by PDADMAC-modified-montmorillonite particle

Dye	Langmuir				Freundlich			Dubinin–Radushkevich		
	Linear form of the isotherm equation: $\dfrac{1}{q_e} + \dfrac{1}{q_m} + \dfrac{1}{K_L C_e q_m}$				Linear form of the isotherm equation: $\ln(q_e) = \ln(K_F) + \dfrac{1}{n}\ln(C_e)$			Linear form of the isotherm equation: $\ln(q_e) = \ln q_m - \beta RT \ln\left(1 + \dfrac{1}{C_e}\right)$		
	K_L (L/mg)	q_m (mg/g)	R_L	R^2	$1/n$	K_F (L/mg)	R^2	β (mol/J)	q_m (mg/g)	R^2
CR	0.756	111.11	0.01	0.9988	0.149	59.38	0.889	7.515×10^{-4}	110.38	0.9535
MO	1.053	100	0.07	0.9995	0.183	43.376	0.836	5.4327×10^{-4}	93.59	0.9483

Table 8
Comparison of CR and MO dyes adsorption on various adsorbents

CR dye			MO dye		
Adsorbent	q_{max} (mg/g)	References	Adsorbent	q_{max} (mg/g)	References
Natural pumice (PN)	3.87	[30]	Na-MMT	24	[54]
Surfactant modified pumice (SMP)	27.32	[30]	Chitosan intercalated montmorillonite	70.42	[55]
Kaolin	5.44	[53]	Alumina nanoparticles	93.3	[46]
Na-Bentonite	35.84	[53]	activated organo-bentonite/ sodium alginate	116	[56]
PDADMAC-modified-montmorillonite	118	This work	PDADMAC-modified-montmorillonite	90	This work
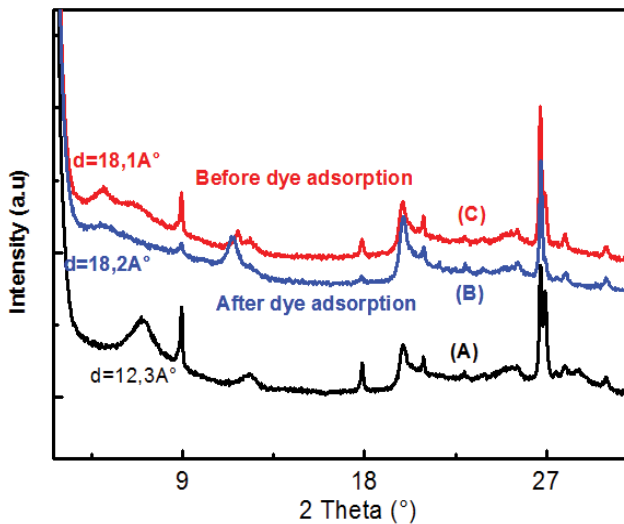
Fig. 11. XRD patterns of unmodified montmorillonite (A), PDADMAC-modified-montmorillonite (C), and PDADMAC-modified-montmorillonite after adsorption of dyes (B).

5. Conclusion

In the present work, the removal of the anionic dyes (CR and MO) from synthetic wastewater was investigated using adsorbent PDADMAC-modified-montmorillonite clay. The adsorption was depending on initial solution pH, temperature, and the interfering anions. In addition, the CR and MO adsorbed amounts onto the PDADMAC-modified-montmorillonite particles were found to decrease with increasing values of solution pH. The rise in temperature of the adsorption medium increases the adsorbed quantities of both dyes. These results suggest that the adsorption of CR and MO dyes onto PDADMAC-modified-montmorillonite solid could be chemisorption. However, decreases in the CR and MO adsorbed amounts were observed upon the increase of the interfering anions (Cl$^-$, SO$_4^{2-}$, CO$_3^{2-}$, and HPO$_4^{2-}$) affinity toward the PDADMAC-modified-montmorillonite surface. The adsorption kinetics of these dyes onto the modified montmorillonite clay is well described by the pseudo-first-order reaction model. Furthermore, the results of CR and MO equilibrium adsorptions onto PDADMAC-modified-montmorillonite materials
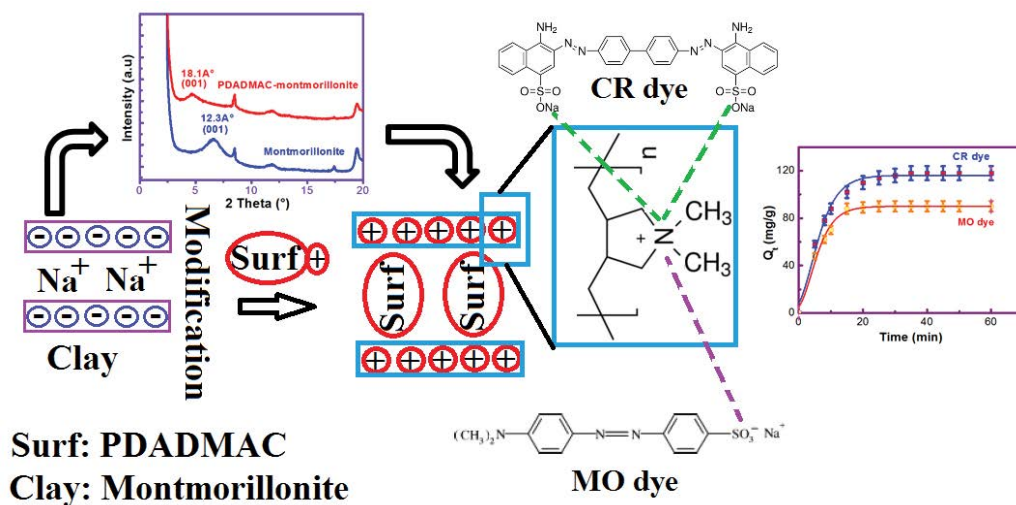
Fig. 12. Conceptual illustration of the proposed mechanism for MO and CR dyes adsorption on PDADMAC-modified montmorillonite.

follow the Langmuir isotherm with a very good correlation coefficient. The PDADMAC-modified-montmorillonite clay particles had adsorption capacity 118 and 90 mg/g for the removal of CR and MO dyes from aqueous solution, respectively.

These results indicate PDADMAC-modified-montmorillonite materials have an important role as potential adsorbent for the efficient removal of dyes normally found in the effluent of various industries.

Acknowledgments

Symbol

R	—	Gas constant, J/mol K
T	—	Temperature, K
t	—	Contact time adsorbate–adsorbent, min
$q(t)$	—	Amount of adsorbate in the adsorbent at any time t, mg/g
q_e	—	Amount of adsorbate in the adsorbent at equilibrium, mg/g
Q, Q_{ads}	—	Adsorbed amount of the solute (the dye) on the solid surface, mg/g
$C_{initial}$	—	Initial concentration of the solute (the dye), mg/L
C_e, C_{eq}	—	Residual concentration of the solute (the dye), mg/L
C_{ste}	—	Constant, mg/g
m_s	—	Amount of the adsorbent solid, g
q_{max}, q_m	—	Maximum adsorption capacity, mg/g
K_L	—	Langmuir equilibrium constant, L/mg
R_L	—	Dimensionless separation constant
K_F	—	Freundlich constant, L/mg
k_1	—	Pseudo-first-order rate constant of adsorption, 1/min
n	—	Freundlich constant, -
k_2	—	Pseudo-second-order rate constant of adsorption, 1/min
K_i	—	Particle diffusion constant, mg/g/min$^{0.5}$
ε	—	Polanyi potential, –
β	—	Constant related to the mean free energy of adsorption, mol^2 kJ^{-2}

References

[1] Z. Huang, Y. Li, W. Chen, J. Shi, N. Zhang, X. Wang, Z. Li, L. Gao, Y. Zhang, Modified bentonite adsorption of organic pollutants of dye wastewater, Mater. Chem. Phys., 202 (2017) 266–276.

[2] C.D. Raman, S. Kanmani, Textile dye degradation using nano zero valent iron: a review, J. Environ. Manage., 177 (2016) 341–355.

[3] S.P. Patil, B. Bethi, G.H. Sonawane, V.S. Shrivastava, S. Sonawane, Efficient adsorption and photocatalytic degradation of Rhodamine B dye over Bi$_2$O$_3$-bentonite nanocomposites: a kinetic study, J. Ind. Eng. Chem., 34 (2016) 356–363.

[4] Y.C. Xu, Z.X. Wang, X.Q. Cheng, Y.C. Xiao, L. Shao, Positively charged nanofiltration membranes via economically mussel-substance-simulated codeposition for textile wastewater treatment, Chem. Eng. J., 303 (2016) 555–564.

[5] S. Olivera, H.B. Muralidhara, K. Venkatesh, V.K. Gunab, K. Gopalakrishna, K.K. Yogesh, Potential applications of cellulose and chitosan nanoparticles/composites in wastewater treatment: a review, Carbohydr. Polym., 153 (2016) 600–618.

[6] S. Dawood, T.K. Sen, Review on dye removal fromits aqueous solution into alternative cost effective and non-conventional adsorbents, J. Chem. Process. Eng., 1 (2013) 1–7.

[7] M. Naushad, G. Sharma, Z.A. Alothman, Photodegradation of toxic dye using Gum Arabic-crosslinkedpoly(acrylamide)/ Ni(OH)$_2$/FeOOH nanocomposites hydrogel, J. Cleaner Prod., 241 (2019) 1182.

[8] N.S. Shaha, J.A. Khan, M. Sayed, Z.U.H. Khan, J. Iqbal, S. Arshad, M. Junaid, H.M. Khan, Synergistic effects of H$_2$O$_2$ and S$_2$O$_8^{2-}$ in the gamma radiation induced degradation of congo-red dye: kinetics and toxicities evaluation, Sep. Purif. Technol., 233 (2020) 1159.

[9] J. Wang, Q. Zhang, X. Shao, J. Ma, G. Tian, Properties of magnetic carbon nanomaterials and application in removal organic dyes, Chemosphere, 207 (2018) 377–384.

[10] V.K. Gupta, R. Jain, A. Mittal, T.A. Saleh, A. Nayak, S. Agarwal, S. Sikarwar, Photo-catalytic degradation of toxic dye amaranth on TiO$_2$/UV in aqueous suspensions, Mater. Sci. Eng., A, 32 (2012) 7–12.

[11] D.P. Dutta, S. Nath, Low cost synthesis of SiO$_2$/C nanocomposite from corn cobs and its adsorption of uranium (VI), chromium (VI) and cationic dyes from wastewater, J. Mol. Liq., 269 (2018) 140–151.

[12] P.S Yap, V. Priyaa, Removal of crystal violet and acid green 25 from water using kaolin, Mater. Sci. Eng., 495 (2019) 12–52.

[13] S. Mallakpour, M. Hatami, An effective, low-cost and recyclable bio-adsorbent having amino acid intercalated LDH@Fe$_3$O$_4$/ PVA magnetic nanocomposites for removal of methyl orange from aqueous solution, Appl. Clay Sci., 174 (2019) 127–137.

[14] M. Baghdadi, B. Alipour Soltani, M. Nourani, Malachite green removal from aqueous solutions using fibrous 2 cellulose sulfate prepared from medical cotton waste: comprehensive 3 batch and column studies, J. Ind. Eng. Chem., 55 (2017) 128–139.

[15] M.A. Ahmad, N.A. Ahmad Puad, O.S. Bello, Kinetic equilibrium and thermodynamic studies of synthetic dye removal using pomegranate peel activated carbon prepared by microwave-induced KOH activation, Water Resour. Ind., 6 (2014) 18–35.

[16] Y. Bentaha, K. Draoui, C. Hurel, O. Ajouyed, S. Khairoun, N. Marmier, Physico-chemical characterization and valorization of swelling and nonswelling Moroccan clays in basic dye removal from aqueous solutions, J. Afr. Earth Sci., 154 (2019) 80–88.

[17] S. Du, L. Wang, N. Xue, M. Pei, W. Sui, W. Guo, Polyethyleneimine modified bentonite for the adsorption of amino black 10B, J. Solid State Chem., 252 (2017) 152–157.

[18] Y. Gao, Y. Guo, H. Zhang, Iron modified bentonite: enhanced adsorption performance for organic pollutant and its regeneration by heterogeneous visible light photo-Fenton process at circumneutral pH, J. Hazard. Mater., 302 (2016) 105–113.

[19] Q. Li, Y. Su, Q. Yue, B. Gao, Adsorption of acid dyes onto bentonite modified with polycations: kinetics study and process design to minimize the contact time, Appl. Clay Sci., 53 (2011) 760–765.

[20] Q. Kang, W. Zhou, Q. Li, B. Gao, J. Fan, D. Shen, Adsorption of anionic dyes on poly(epicholorohydrin dimethylamine) modified bentonite in single and mixed dye solutions, Appl. Clay Sci., 45 (2009) 280–287.

[21] Y. Liu, Y. Kang, B. Mu, A. Wang, Attapulgite/bentonite interactions for methylene blue adsorption characteristics from aqueous solution, Chem. Eng. J., 237 (2014) 403–410.

[22] S.L. Bartelt-Hunt, S.E. Burns, J.A Smith, Nonionic organic solute sorption to two organobentonites as a function of organic-carbon content, J. Colloid Interface Sci., 266 (2003) 251–258.

[23] A. Khenifi, B. Zohra, B. Kahina, H. Houari, D. Zoubir, Removal of 2,4-DCP from wastewater by CTAB/bentonite using one – step and two-step methods: a comparative study, Chem. Eng. J., 146 (2009) 345–354.

[24] R.S. Juang, F.C. Wu, R.L. Tseng, Mechanism of adsorption of dyes and phenols from water using activated carbons prepared from plum kernels, J. Colloid Interface Sci., 227 (2000) 437–444.

[25] F.E. Titchou, R. Ait Akbour, A. Assabbane, M. Hamdani, Removal of cationic dye from aqueous solution using Moroccan pozzolana as adsorbent: isotherms, kinetic studies, and application on real textile wastewater treatment, Groundwater Sustainable Dev., 11 (2020) 1004.

[26] H. Lata, V.K. Garg, R.K. Gupta, Adsorptive removal of basic dye by chemically activated Parthenium biomass: equilibrium and kinetic modeling, Desalination, 219 (2008) 250–261.

[27] A. Belaroussi, F. Labed, A. Khenifi, R. Ait Akbour, Z. Bouberka, M. Kameche, Z. Derriche, A novel approach for removing an industrial dye 4GL by an Algerian Bentonite, Acta Ecol. Sin., 38 (2018) 148–156.

[28] Z. Luo, M. Gao, Y. Ye, S. Yang, Modification of reduced-charge montmorillonites by a series of Gemini surfactants: characterization and application in methyl orange removal, Appl. Surf. Sci., 324 (2015) 807–816.

[29] V.K. Gupta, D. Mohan, V.K. Saini, Studies on the interaction of some azo dyes (naphthol red-J and direct orange) with nontronite mineral, J. Colloid Interface Sci., 298 (2006) 79–86.

[30] H. Shayesteh, A. Rahbar-Kelishami, R. Norouzbeigi, Evaluation of natural and cationic surfactant modified pumice for Congo red removal in batch mode: kinetic, equilibrium, and thermodynamic studies, J. Mol. Liq., 221 (2016) 1–11.

[31] L. Zhou, H. Chen, X. Jiang, F. Lu, Y. Zhou, W. Yin, X. Ji, Modification of montmorillonite surfaces using a novel class of cationic gemini surfactants, J. Colloid Interface Sci., 332 (2009) 16–21.

[32] H. Ren, S. Tian, M. Zhu, Y. Zhao, K. Li, Q. Ma, S. Ding, J. Gao, Z. Miao, Modification of montmorillonite by Gemini surfactants with different chain lengths and its adsorption behavior for methyl orange, Appl. Clay Sci., 151 (2018) 29–36.

[33] J.M. Cases, F. Villieras, Thermodynamic model of ionic and nonionic surfactant adsorption–abstraction on heterogeneous surfaces, Langmuir, 8 (1992) 1251–1264.

[34] S. Yang, M. Gao, Z. Luo, Adsorption of 2-naphthol on the organo-montmorillonites modified by Gemini surfactants with different spacers, Chem. Eng. J., 256 (2014) 39–50.

[35] L. Yan, L. Qin, H. Yu, S. Li, R. Shan, B. Du, Adsorption of acid dyes from aqueous solution by CTMAB modified bentonite: kinetic and isotherm modeling, J. Mol. Liq., 211 (2015) 1074–1081.

[36] M. Boufatit, H. Ait-Amar, W.R. McWhinnie, Development of an Algerian material montmorillonite clay. Adsorption of phenol, 2-dichlorophenol and 2,4,6-trichlorophenol fromaqueous solutions onto montmorillonite exchanged with transition metal complexes, Desalination, 206 (2007) 394–406.

[37] Z. Huang, Y. Li, W. Chen, J. Shi, N. Zhang, X. Wang, Z. Li, L. Gao, Y. Zhang, Formulation study for softening of hard water using surfactant modified bentonite adsorbent coating, Mater. Chem. Phys., 202 (2017) 266–276.

[38] Y.S. Ho, Citation review of Lagergren kinetic rate equation on adsorption reactions, Sientometrics, 59 (2004) 171–177.

[39] Y.S. Ho, G. McKay, The kinetics of sorption of divalent metal ions onto sphagnum moss peat, Water Res., 34 (2000) 735–742.

[40] J. Shah, M. Rasul Jan, M. Zeeshan, M. Imran, Kinetic, equilibrium and thermodynamic studies for sorption of 2,4-dichlorophenol onto surfactant modified fuller's earth, Appl. Clay Sci., 143 (2017) 227–233.

[41] S. Nethaji, A. Sivasamy, A.B. Mandal, Adsorption isotherms, kinetics and mechanism for the adsorption of cationic and anionic dyes onto carbonaceous particles prepared from Juglans regia shell biomass, Int. J. Environ. Sci. Technol., 10 (2013) 231–242.

[42] C.Y. Cao, L.K. Meng, Y.H. Zhao, Adsorption of phenol from wastewater by organo-bentonite, Desal. Water Treat., 52 (2014) 3504–3509.

[43] A. Ozcan, C. Omeroğlu, Y. Erdoğan, A.S. Ozcan, Modification of bentonite with a cationic surfactant: adsorption study of textile dye Reactive Blue 19, J. Hazard. Mater., 140 (2007) 173–179.

[44] B.H. Hameed, A.A. Ahmad, N. Aziz, Adsorption of reactive dye on palm-oil industry waste: equilibrium, kinetic and thermodynamic studies, Desalination, 247 (2009) 551–560.

[45] D. Shen, J. Fan, W. Zhou, B. Gao, Q. Yue, Q. Kang, Adsorption kinetics and isotherm of anionic dyes onto organo-bentonite from single and multisolute systems, J. Hazard. Mater., 172 (2009) 99–107.

[46] S. Banerjee, S. Dubey, R. Kumar Gautam, M.C. Chattopadhyaya, Y.C. Sharma, Adsorption characteristics of alumina nano-particles for the removal of hazardous dye, Orange G from aqueous solutions, Arabian J. Chem., 12 (2019) 5339–5354.

[47] C.A.P. Almeida, N.A. Debacher, A.J. Downs, L. Cottet, C.A.D. Mello, Removal of methylene blue from colored effluent by adsorption on montmorillonite clay, J. Colloid Interface Sci., 332 (2009) 46–53.

[48] L. Wang, A. Wang, Adsorption properties of Congo Red from aqueous solution onto surfactant-modified montmorillonite, J. Hazard. Mater., 160 (2008) 173–180.

[49] C.H. Giles, T.H. McEwan, S.N. Nakhwa, Smith, Studies in adsorption. XI. A system of classification of solution adsorption isotherms and its use in diagnosis of adsorption mechanisms and in measurements of specific areas of soils, J. Chem. Soc., 786 (1960) 3973–3993.

[50] I. Langmuir, The adsorption of gases on plane surfaces of glass, mica and platinum, J. Am. Chem. Soc., 40 (1918) 1361–1403.

[51] H.M.F. Freundlich, Over the adsorption in solution, J. Phys. Chem., 57 (1906) 385–471.

[52] M.M. Dubinin, L.V. Radushkevich, The equation of the characteristic cuves of the activated charcoal, Chem. Sec., 55 (1947) 331–337.

[53] V. Vimonses, S. Lei, B. Jin, C.W.K. Chow, C. Saint, Kinetic study and equilibrium isotherm analysis of Congo Red adsorption by clay materials, Chem. Eng. J., 148 (2009) 354–364.

[54] D. Chen, J. Chen, X. Luan, H. Ji, Z. Xia, Characterization of anion–cationic surfactants modified montmorillonite and its application for the removal of methyl orange, Chem. Eng. J., 171 (2011) 1150–1158.

[55] C. Umpuch, S. Sakaew, Removal of methyl orange from aqueous solutions by adsorption using chitosan intercalated montmorillonite, Songklanakarin J. Sci. Technol., 35 (2013) 451–459.

[56] N. Belhouchat, H. Zaghouane-Boudiaf, C. Viseras, Removal of anionic and cationic dyes from aqueous solution with activated organo-bentonite/sodium alginate encapsulated beads, Appl. Clay Sci., 135 (2016) 9–15.